



Article

Paramarkeyite, a new calcium–uranyl–carbonate mineral from the Markey mine, San Juan County, Utah, USA

Anthony R. Kampf^{1*} , Travis A. Olds², Jakub Plášil³ , Peter C. Burns⁴, Radek Škoda⁵ and Joe Marty¹

¹Mineral Sciences Department, Natural History Museum of Los Angeles County, 900 Exposition Boulevard, Los Angeles, CA 90007, USA; ²Section of Minerals and Earth Sciences, Carnegie Museum of Natural History, 4400 Forbes Avenue, Pittsburgh, Pennsylvania 15213, USA; ³Institute of Physics ASCR, v.v.i., Na Slovance 1999/2, 18221 Prague 8, Czech Republic; ⁴Department of Civil and Environmental Engineering and Earth Sciences, Department of Chemistry and Biochemistry, University of Notre Dame, Notre Dame, IN 46556, USA; and ⁵Department of Geological Sciences, Faculty of Science, Masaryk University, Kotlářská 2, 611 37, Brno, Czech Republic

Abstract

The new mineral paramarkeyite (IMA2021-024), $\text{Ca}_2(\text{UO}_2)(\text{CO}_3)_3 \cdot 5\text{H}_2\text{O}$, was found in the Markey mine, San Juan County, Utah, USA, where it occurs as a secondary phase on gypsum-coated asphaltum in association with andersonite, calcite, gypsum and natromarkeyite. Paramarkeyite crystals are transparent, pale green-yellow, striated tablets, up to 0.11 mm across. The mineral has white streak and vitreous lustre. It exhibits moderate bluish-white fluorescence (405 nm laser). It is very brittle with irregular, curved fracture and a Mohs hardness of 2½. It has an excellent {100} cleavage and probably two good cleavages on {010} and {001}. The measured density is 2.91(2) g cm⁻³. Optically, the mineral is biaxial (–) with $\alpha = 1.550(2)$, $\beta = 1.556(2)$, $\gamma = 1.558(2)$ (white light); $2V = 60(2)^\circ$; strong $r > v$ dispersion; orientation: $Y = \mathbf{b}$; nonpleochroic. The Raman spectrum exhibits bands consistent with UO_2^{2+} , CO_3^{2-} and O–H. Electron microprobe analysis provided the empirical formula $(\text{Ca}_{1.83}\text{Na}_{0.20}\text{Sr}_{0.03})_{\Sigma 2.05}(\text{UO}_2)(\text{CO}_3)_3 \cdot 5\text{H}_2\text{O}$ (+0.07 H). Paramarkeyite is monoclinic, $P2_1/n$, $a = 17.9507(7)$, $b = 18.1030(8)$, $c = 18.3688(13)$ Å, $\beta = 108.029(8)^\circ$, $V = 5676.1(6)$ Å³ and $Z = 16$. The structure of paramarkeyite ($R_1 = 0.0647$ for 6657 $I > 2\sigma I$) contains uranyl tricarbonate clusters that are linked by Ca–O polyhedra to form heteropolyhedral layers. The structure of paramarkeyite is very similar to those of markeyite, natromarkeyite and pseudomarkeyite.

Keywords: paramarkeyite, new mineral, uranyl tricarbonate, crystal structure, markeyite, natromarkeyite, pseudomarkeyite, Markey mine, Utah, USA

(Received 6 September 2021; accepted 6 December 2021; Accepted Manuscript published online: 13 December 2021; Associate Editor: Giancarlo Della Ventura)

Introduction

The Blue Lizard, Green Lizard, Giveaway–Simplot and Markey mines in the Red Canyon portion of the White Canyon district in south-eastern Utah have yielded many new mineral species in recent years (e.g. Kampf *et al.*, 2021a). Most of the new species are uranyl sulfates and most, especially from the Blue Lizard mine, contain Na. Of the ten new species that the Markey mine has yielded, all contain uranyl and six contain carbonate; of the six new uranyl carbonates, five also contain essential Ca. The new mineral paramarkeyite, which is included in the aforementioned enumerations, is very closely related to three of the other new minerals from the Markey mine: markeyite (Kampf *et al.*, 2018), natromarkeyite and pseudomarkeyite (Kampf *et al.*, 2020a).

A preponderance of uranyl carbonate minerals form structures based on finite clusters of polyhedra that have relatively weak bonding interactions (~0.1–0.4 vu) between bridging and non-bridging cations and carbonate polyhedra (Lussier *et al.*, 2016). The uranyl tricarbonate (UTC) unit, $[(\text{UO}_2)(\text{CO}_3)_3]^{4-}$,

present in most of the currently known uranyl carbonate minerals is highly stable and only slight differences in pH and cation: U:CO₃ content affects uranyl carbonate speciation in solution, leading to crystallisation of a wide variety of finite cluster-based topologies. Likewise, numerous uranyl sulfate minerals based on finite cluster topologies (especially those found in Red Canyon) crystallise relatively rapidly as efflorescent crusts from high ionic-strength solutions, suggesting that the aqueous conformation of polyhedral clusters may be retained from solution to crystal.

Paramarkeyite (IMA2021-024, Kampf *et al.*, 2021b) is named based on the Greek $\pi\alpha\rho\alpha$ for ‘near’ and the mineral markeyite to which it is similar. It is also similar to natromarkeyite and pseudomarkeyite. The four minerals are similar in appearance, composition, Raman spectrum and structure. Note that markeyite (/ma:r 'ki: ait/) is named for the locality, the Markey mine. The new mineral and name were approved by the Commission on New Minerals, Nomenclature and Classification of the International Mineralogical Association. The description is based on two cotype specimens deposited in the collections of the Natural History Museum of Los Angeles County, 900 Exposition Boulevard, Los Angeles, CA 90007, USA, catalogue numbers 67487 and 67488; 67487 is also the holotype for natromarkeyite and 67488 is also the cotype for natromarkeyite.

*Author for correspondence: Anthony R. Kampf, Email: akampf@nhm.org

Cite this article: Kampf A.R., Olds T.A., Plášil J., Burns P.C., Škoda R. and Marty J. (2022) Paramarkeyite, a new calcium–uranyl–carbonate mineral from the Markey mine, San Juan County, Utah, USA. *Mineralogical Magazine* 86, 27–36. <https://doi.org/10.1180/mgm.2021.100>

Occurrence

Paramarkeyite was found underground in the Markey mine, Red Canyon, White Canyon District, San Juan County, Utah, USA (37°32'57"N, 110°18'08"W). The Markey mine is located ~1 km southwest of the Blue Lizard mine, on the east-facing side of Red Canyon, ~72 km west of the town of Blanding, Utah, and ~22 km southeast of Good Hope Bay on Lake Powell. The geology of the Markey mine is quite similar to that of the Blue Lizard mine (Chenoweth, 1993; Kampf *et al.*, 2017), although the secondary mineralogy of the Markey mine is notably richer in carbonate phases. Underground gas measurements collected in 2016 using a hand-held Crowcon Gasman CO₂ monitor showed consistently elevated CO₂ levels at the Markey mine, averaging ~1000 ppm CO₂ with a maximum recorded value of 1600 ppm CO₂, levels considerably higher than at the nearby Blue Lizard mine where carbonate mineral species are less abundant. Higher CO₂ concentration at the Markey mine may be connected to an abundance of calcite present in the ores, released by the action of acidic waters derived from decaying sulfides.

The following information regarding the history and geology is taken largely from Chenoweth (1993). Jim Rigg of Grand Junction, Colorado began staking claims in Red Canyon in March of 1949. The Markey group of claims, staked by Rigg and others, was purchased by the Anaconda Copper Mining Company on June 1, 1951. After limited exploration and production, the mine closed in 1955. The mine was subsequently acquired from Anaconda by Calvin Black of Blanding, Utah under whose ownership the mine operated from 1960 to 1982 and was a leading producer in the district for nearly that entire period.

The uranium deposits in Red Canyon occur within the Shinarump member of the Upper Triassic Chinle Formation, in channels incised into the reddish-brown siltstones of the underlying Lower Triassic Moenkopi Formation. The Shinarump member consists of medium- to coarse-grained sandstone, conglomeratic sandstone beds and thick siltstone lenses. Ore minerals (uraninite, montroseite, coffinite, etc.) were deposited as replacements of wood and other organic material and as disseminations in the enclosing sandstone. Since the mine closed in 1982, oxidation of primary ores in the humid underground environment has produced a variety of secondary minerals, mainly carbonates and sulfates, as efflorescent crusts on the surfaces of mine walls.

Paramarkeyite is a very rare mineral in the secondary mineral assemblage at the Markey mine. It occurs on gypsum-coated asphaltum in association with andersonite, calcite, gypsum and natromarkeyite (Kampf *et al.*, 2020a). Other new minerals recently described from the Markey mine are feynmanite (Kampf *et al.*, 2019a), leószilárdite (Olds *et al.*, 2017), magnesioleydetite (Kampf *et al.*, 2019b), markeyite (Kampf *et al.*, 2018), meyrowitzite (Kampf *et al.*, 2019c), pseudomarkeyite (Kampf *et al.*, 2020a), straßmannite (Kampf *et al.*, 2019b) and uroxite (Kampf *et al.*, 2020b).

Physical and optical properties

Paramarkeyite crystals are striated tablets (Fig. 1) up to ~0.11 mm across, commonly in parallel intergrowths. Tablets are probably flattened on {100} and striated parallel to [010] and [001]; however, because crystals occur in parallel intergrowths and easily

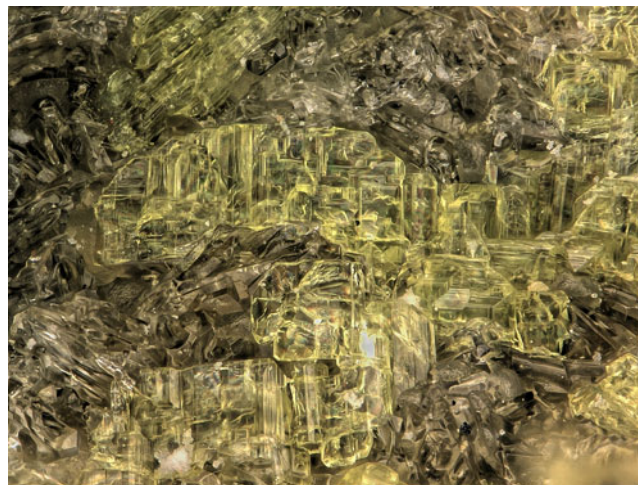


Fig. 1. Paramarkeyite on gypsum; field of view 0.84 mm across (catalogue number 67487).

break into irregular fragments, it was not possible to extract complete crystals for measurements. The morphological description is based, in part, on the structure of paramarkeyite by analogy with relation of morphology to structure in the closely related minerals markeyite, natromarkeyite and pseudomarkeyite. The forms {100}, {010}, {001}, {110}, {101}, {10 $\bar{1}$ } and {011} (Fig. 2) are based upon observed morphology, but were not measured. No twinning was observed.

Crystals are pale green yellow and transparent with vitreous lustre. The streak is white. The mineral fluoresces moderate bluish white under a 405 nm laser. The Mohs hardness is 2½, based upon scratch tests. Crystals are very brittle with irregular, curved fracture. There is excellent cleavage on {100}, and probably two good cleavages on {010} and {001}. In room-temperature H₂O, the mineral slowly loses birefringence, but does not dissolve; it dissolves immediately with effervescence in dilute HCl. The density measured by flotation in a mixture of methylene iodide and toluene is 2.91(2) g cm⁻³. The calculated density based on the empirical formula and unit-cell parameters obtained from single-crystal X-ray diffraction data is 2.905 g cm⁻³.

Optically, paramarkeyite is biaxial (-), with $\alpha = 1.550(2)$, $\beta = 1.556(2)$, $\gamma = 1.558(2)$ (measured in white light). The 2V

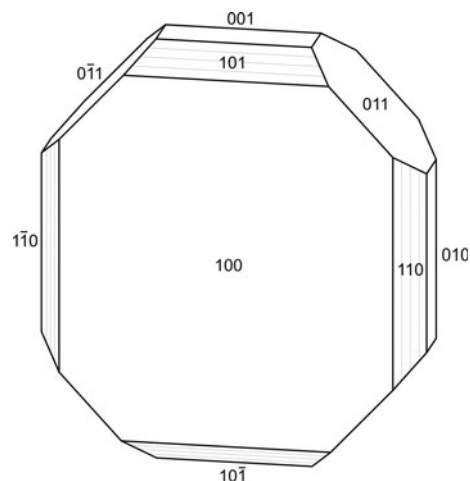


Fig. 2. Crystal drawing of paramarkeyite; clinographic projection.

measured directly on a spindle stage is $60(2)^\circ$; the calculated $2V$ is 59.8° . Dispersion is $r > v$, strong. The mineral is nonpleochroic. The partially determined optical orientation is $Y = \mathbf{b}$. The Gladstone–Dale compatibility index $1 - (K_p/K_c)$ for the empirical formula is -0.025 , in the excellent range (Mandarino, 2007), using $k(\text{UO}_3) = 0.118$, as provided by Mandarino (1976).

Raman spectroscopy

A Raman spectrum was collected from a loose crystal fragment of paramarkeyite using a Horiba LabRAM HR Evolution spectrometer equipped with a 532 nm diode laser. The Raman spectrum of paramarkeyite is very similar to those of markeyite (Kampf *et al.*, 2017), natromarkeyite (Kampf *et al.*, 2020a) and pseudomarkeyite (Kampf *et al.*, 2020a). All four spectra are compared in Fig. 3.

Multiple broad bands in the $3700\text{--}3100\text{ cm}^{-1}$ range are attributed to ν O–H stretching vibrations of symmetrically distinct hydrogen-bonded H_2O groups. According to the correlation given by Libowitzky (1999), this corresponds to approximate O–H...O hydrogen bond-lengths between 3.2 and 2.7 Å, which is consistent with what is reported in the structures of markeyite and pseudomarkeyite. The broad bands in the $2800\text{--}2300\text{ cm}^{-1}$ range in the markeyite and pseudomarkeyite spectra were originally interpreted as corresponding to strong (short) hydrogen

Table 1. Chemical composition (in wt.%) for paramarkeyite.

| Constituent | Mean | Range | S.D. | Standard |
|------------------------|--------|-------------|------|----------------------|
| Na_2O | 1.05 | 0.78–1.21 | 0.15 | albite |
| CaO | 17.06 | 16.77–17.43 | 0.23 | fluorapatite |
| SrO | 0.46 | 0.30–0.63 | 0.14 | syn. SrSO_4 |
| UO_3 | 47.44 | 46.64–49.14 | 0.91 | syn. UO_2 |
| CO_2^* | 21.90 | | | |
| H_2O^* | 15.05 | | | |
| Total | 102.96 | | | |

* Based on the structure. S.D. – standard deviation.

bonds (Kampf *et al.*, 2018); however, no such bands appear to exist in these structures and no such bands are seen in the paramarkeyite spectrum. We now think that these may be spectral artefacts because such bands have also been observed in spectra of anhydrous minerals, and we have recorded other spectra for markeyite that do not exhibit this feature.

The weak bands between ~ 1450 and 1300 cm^{-1} can be attributed to the $\nu_3(\text{CO}_3)^{2-}$ antisymmetric stretching vibrations of the $(\text{CO}_3)^{2-}$ units. Medium to strong multiple bands between 1100 and 1050 cm^{-1} are connected with the $\nu_1(\text{CO}_3)^{2-}$ symmetric stretching vibrations of several structurally non-equivalent carbonate units (Koglin *et al.*, 1979; Anderson *et al.*, 1980; Čejka, 1999 and 2005).

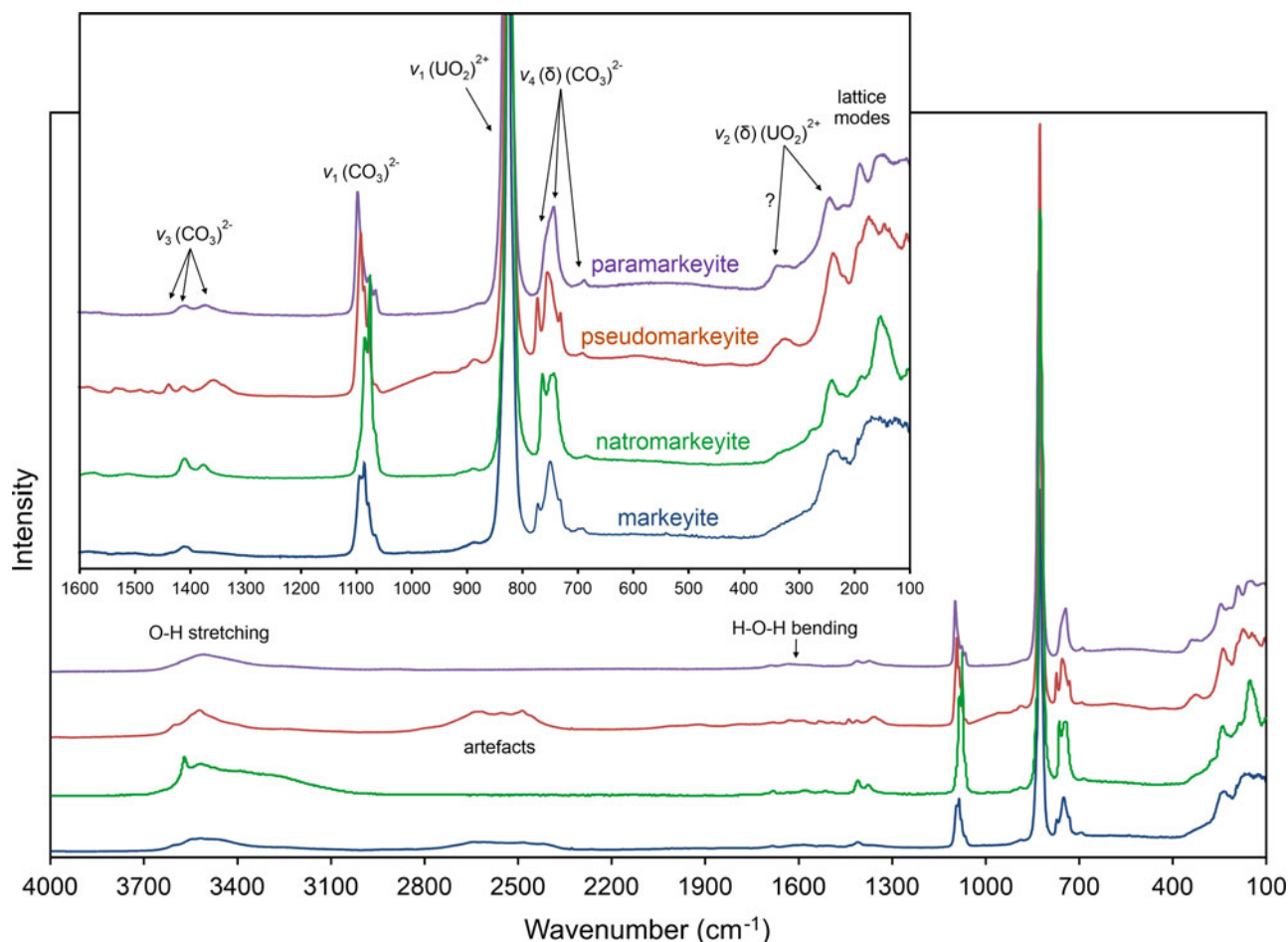


Fig. 3. Comparison of the Raman spectra of paramarkeyite, pseudomarkeyite, natromarkeyite and markeyite.

Table 2. Data collection and structure refinement details for paramarkeyite.*

| Crystal data | |
|--|---|
| Structural formula | (Ca _{1.76} Na _{0.21} Sr _{0.03})Σ _{2.00} (UO ₂)(CO ₃) ₃ ·4.55H ₂ O (including unlocated H) |
| Space group | <i>P</i> 2 ₁ / <i>n</i> |
| Unit cell dimensions (Å, °) | <i>a</i> = 17.9507(7) <i>b</i> = 18.1030(8) <i>c</i> = 18.3688(13) β = 108.029(8) |
| <i>V</i> (Å ³) | 5676.1(6) |
| <i>Z</i> | 16 |
| Density (for above formula) (g·cm ⁻³) | 2.856 |
| Absorption coefficient (mm ⁻¹) | 12.272 |
| Data collection | |
| Diffractometer | Rigaku R-Axis Rapid II |
| X-ray radiation/power | MoKα (λ = 0.71075 Å)/50 kV, 40 mA |
| Temperature (K) | 293(2) |
| Crystal size (μm) | 110 × 90 × 80 |
| <i>F</i> (000) | 4514.8 |
| θ range (°) | 2.99 to 25.03 |
| Index ranges | -21 ≤ <i>h</i> ≤ 21, -21 ≤ <i>k</i> ≤ 21, -21 ≤ <i>l</i> ≤ 21 |
| Reflections collected/unique | 39155/9933; <i>R</i> _{int} = 0.097 |
| Reflections with <i>I</i> > 2σ | 6657 |
| Completeness to θ = 25.03° | 99.1% |
| Refinement | |
| Refinement method | Full-matrix least-squares on <i>F</i> ² |
| Parameters/restraints | 788/0 |
| GoF | 1.030 |
| Final <i>R</i> indices [<i>F</i> > 4σ(<i>F</i>)] | <i>R</i> ₁ = 0.0647, <i>wR</i> ₂ = 0.1291 |
| <i>R</i> indices (all data) | <i>R</i> ₁ = 0.1040, <i>wR</i> ₂ = 0.1472 |
| Largest diff. peak/hole (e ⁻ ·Å ⁻³) | +1.77/-1.88 |

**R*_{int} = Σ|*F*_o - *F*_c(mean)|/Σ|*F*_o|. GoF = $S = \frac{\sum[w(F_o^2 - F_c^2)^2]}{\sum(F_o^2)}$. $R_1 = \frac{\sum||F_o| - |F_c||}{\sum|F_o|}$. $wR_2 = \frac{\sum[w(F_o^2 - F_c^2)^2]}{\sum[w(F_o^2)^2]}$; $w = 1/[\sigma^2(F_o^2) + (aP)^2 + bP]$ where *a* is 0.0337, *b* is 176.6 and *P* is $[2F_o^2 + \text{Max}(F_o^2, 0)]/3$.

The very strong bands centred at 826, 827, 829 and 830 cm⁻¹ for markeyite, pseudomarkeyite, natromarkeyite and paramarkeyite, respectively, are due to the ν₁ (UO₂)²⁺ symmetric stretching vibrations and provide inferred U–O bond lengths of ~1.78–1.79 Å (Bartlett and Cooney, 1989). The ν₂ (δ) (CO₃)²⁻ bending vibration may coincide with this band.

Several weak to strong bands in the range 780 to 680 cm⁻¹ are assigned to the doubly degenerate ν₄ (δ) (CO₃)²⁻ bending vibrations. The medium-strength band in the spectra centred near 240 cm⁻¹ is assigned to the split doubly degenerate ν₂ (δ) (UO₂)²⁺ bending vibrations. Bands between 200 and 120 cm⁻¹ are due to lattice modes (Koglin *et al.*, 1979; Anderson *et al.*, 1980; Čejka, 1999 and 2005).

Chemical composition

Chemical analyses (6) were performed using a Cameca SX100 electron microprobe at Masaryk University, Brno, operating in wavelength dispersive spectroscopy mode using an accelerating voltage of 15 kV, beam current of 1 nA and a 15 μm beam diameter. Such mild conditions were used in order to minimise the decomposition of the analysed area by the electron beam. The analysed area showed no visible changes in back-scattered electron spectroscopy or reflected light after the analysis. Concentrations of elements other than those reported in Table 1 were below detection limits. Matrix correction by the X-PHI algorithm (Merlet, 1994) was applied to the data. Insufficient material was available for CHN analysis; however, the fully ordered structure and detailed bond-valence analysis unambiguously established the identities of O, H₂O and CO₂ and the corresponding quantitative contents of H₂O and CO₂,

Table 3. Atom coordinates and displacement parameters (Å²) for paramarkeyite.

| | Occupancy | <i>x/a</i> | <i>y/b</i> | <i>z/c</i> | <i>U</i> _{eq} | <i>U</i> ¹¹ | <i>U</i> ²² | <i>U</i> ³³ | <i>U</i> ²³ | <i>U</i> ¹³ | <i>U</i> ¹² |
|-----|-----------|-------------|-------------|-------------|------------------------|------------------------|------------------------|------------------------|------------------------|------------------------|------------------------|
| Ca1 | 1 | 0.18284(18) | 0.37177(18) | 0.66149(17) | 0.0244(7) | 0.0294(17) | 0.0233(19) | 0.0245(17) | -0.0004(14) | 0.0142(13) | -0.0006(14) |
| Ca2 | 1 | 0.02897(18) | 0.18262(19) | 0.42745(17) | 0.0263(7) | 0.0352(17) | 0.0238(18) | 0.0210(16) | -0.0012(14) | 0.0101(13) | 0.0026(15) |
| Ca3 | 1 | 0.9746(2) | 0.3178(2) | 0.6983(2) | 0.0415(9) | 0.053(2) | 0.029(2) | 0.059(2) | 0.0034(19) | 0.0414(19) | 0.0023(19) |
| Ca4 | 1 | 0.16711(18) | 0.37337(18) | 0.28051(17) | 0.0242(7) | 0.0295(17) | 0.0233(19) | 0.0227(17) | 0.0005(14) | 0.0125(13) | -0.0004(14) |
| Ca5 | 1 | 0.17432(18) | 0.99695(19) | 0.67354(17) | 0.0253(7) | 0.0280(17) | 0.027(2) | 0.0238(17) | 0.0014(14) | 0.0124(13) | -0.0005(14) |
| Ca6 | 1 | 0.17782(18) | 0.99667(18) | 0.30010(17) | 0.0256(7) | 0.0318(17) | 0.0245(19) | 0.0239(17) | 0.0008(14) | 0.0136(14) | 0.0008(15) |
| Ca7 | 0.54(2) | 0.4706(7) | 0.5520(7) | 0.5489(5) | 0.067(5) | 0.096(9) | 0.072(9) | 0.046(5) | -0.017(5) | 0.040(5) | -0.040(8) |
| Na7 | 0.46(2) | 0.4267(8) | 0.6023(9) | 0.5381(7) | 0.022(4) | 0.023(8) | 0.021(10) | 0.015(7) | 0.009(6) | -0.003(5) | -0.009(7) |
| Ca8 | 0.50 | 0.4703(6) | 0.1609(9) | 0.6146(6) | 0.105(5) | 0.073(7) | 0.185(15) | 0.062(7) | 0.025(8) | 0.029(5) | 0.068(8) |
| Na8 | 0.38 | 0.5089(12) | 0.1868(19) | 0.5422(15) | 0.100(11) | 0.037(12) | 0.16(3) | 0.090(19) | -0.053(19) | 0.000(12) | 0.035(15) |
| Sr9 | 0.120(7) | 0.9202(10) | 0.4938(10) | 0.4961(10) | 0.058(7) | 0.061(12) | 0.054(13) | 0.059(12) | -0.001(9) | 0.019(9) | 0.031(9) |
| U1 | 1 | 0.30311(3) | 0.18496(4) | 0.74340(3) | 0.02935(17) | 0.0295(3) | 0.0255(4) | 0.0314(4) | 0.0010(3) | 0.0071(3) | -0.0015(3) |
| U2 | 1 | 0.26117(4) | 0.44481(4) | 0.49624(4) | 0.0412(2) | 0.0505(4) | 0.0530(5) | 0.0236(3) | -0.0049(3) | 0.0167(3) | -0.0257(4) |
| U3 | 1 | 0.27321(4) | 0.92870(4) | 0.51515(3) | 0.0395(2) | 0.0362(4) | 0.0624(5) | 0.0247(3) | 0.0076(3) | 0.0165(3) | 0.0172(4) |
| U4 | 1 | 0.27655(4) | 0.18521(4) | 0.26438(5) | 0.0464(2) | 0.0544(4) | 0.0238(4) | 0.0825(6) | 0.0078(4) | 0.0524(4) | 0.0054(4) |
| C1 | 1 | 0.3624(10) | 0.0427(11) | 0.8106(10) | 0.038(4) | 0.031(10) | 0.041(13) | 0.046(11) | -0.010(10) | 0.016(8) | -0.017(9) |
| C2 | 1 | 0.1559(9) | 0.1863(10) | 0.6193(9) | 0.031(4) | 0.038(9) | 0.030(10) | 0.026(9) | 0.002(8) | 0.011(7) | -0.011(9) |
| C3 | 1 | 0.3728(9) | 0.3259(10) | 0.8030(9) | 0.031(4) | 0.027(9) | 0.027(11) | 0.035(10) | 0.008(8) | 0.004(7) | -0.002(8) |
| C4 | 1 | 0.1281(9) | 0.3492(9) | 0.4584(8) | 0.027(4) | 0.042(10) | 0.028(10) | 0.011(8) | 0.004(7) | 0.010(7) | 0.021(8) |
| C5 | 1 | 0.3348(8) | 0.4938(10) | 0.6515(9) | 0.028(4) | 0.015(8) | 0.042(11) | 0.029(9) | 0.006(8) | 0.008(7) | -0.021(7) |
| C6 | 1 | 0.3308(13) | 0.4828(14) | 0.3799(12) | 0.071(8) | 0.083(16) | 0.091(19) | 0.042(13) | -0.008(12) | 0.022(11) | -0.072(15) |
| C7 | 1 | 0.1336(10) | 0.0172(10) | 0.4745(10) | 0.038(4) | 0.039(10) | 0.040(12) | 0.038(11) | -0.013(9) | 0.018(9) | -0.021(9) |
| C8 | 1 | 0.1605(12) | 0.3815(13) | 0.8271(10) | 0.058(6) | 0.075(14) | 0.086(18) | 0.022(10) | 0.010(11) | 0.026(10) | -0.040(13) |
| C9 | 1 | 0.3477(10) | 0.8928(12) | 0.4021(10) | 0.047(5) | 0.033(10) | 0.076(16) | 0.035(11) | 0.018(10) | 0.016(8) | 0.015(10) |
| C10 | 1 | 0.1338(10) | 0.1847(10) | 0.3034(10) | 0.039(4) | 0.039(10) | 0.025(10) | 0.059(12) | -0.012(9) | 0.025(9) | -0.003(9) |
| C11 | 1 | 0.8412(11) | 0.1817(13) | 0.7302(11) | 0.049(5) | 0.052(12) | 0.046(14) | 0.060(13) | 0.004(11) | 0.032(10) | -0.002(11) |
| C12 | 1 | 0.3541(11) | 0.0500(10) | 0.2522(12) | 0.049(5) | 0.064(13) | 0.014(10) | 0.096(16) | 0.004(10) | 0.064(12) | -0.003(10) |
| O1 | 1 | 0.1180(7) | 0.4859(7) | 0.6547(7) | 0.045(3) | 0.039(7) | 0.029(8) | 0.062(9) | -0.019(7) | 0.008(6) | 0.004(6) |
| O2 | 1 | 0.2966(6) | 0.0500(6) | 0.7555(6) | 0.035(3) | 0.042(7) | 0.019(7) | 0.039(7) | -0.006(5) | 0.003(5) | 0.000(5) |
| O3 | 1 | 0.4022(7) | 0.1039(7) | 0.8256(7) | 0.044(3) | 0.043(7) | 0.023(7) | 0.058(8) | 0.012(6) | 0.002(6) | 0.010(6) |
| O4 | 1 | 0.0915(6) | 0.1870(6) | 0.5676(6) | 0.030(3) | 0.029(6) | 0.031(7) | 0.020(6) | -0.005(5) | -0.005(5) | -0.004(5) |

(Continued)

Table 3. (Continued.)

| | Occupancy | x/a | y/b | z/c | U_{eq} | U^{11} | U^{22} | U^{33} | U^{23} | U^{13} | U^{12} |
|------|-----------|------------|------------|------------|-----------|-----------|-----------|-----------|------------|-----------|------------|
| O5 | 1 | 0.1955(6) | 0.2451(6) | 0.6469(6) | 0.037(3) | 0.034(6) | 0.024(7) | 0.044(7) | -0.003(6) | -0.004(5) | 0.008(5) |
| O6 | 1 | 0.1912(6) | 0.1250(6) | 0.6520(6) | 0.030(3) | 0.022(6) | 0.023(7) | 0.039(7) | 0.004(5) | 0.001(5) | -0.002(5) |
| O7 | 1 | 0.4034(6) | 0.3846(6) | 0.8359(6) | 0.034(3) | 0.036(6) | 0.020(7) | 0.041(7) | -0.004(5) | 0.004(5) | -0.004(5) |
| O8 | 1 | 0.4067(6) | 0.2635(6) | 0.8236(6) | 0.032(3) | 0.035(6) | 0.022(7) | 0.032(6) | -0.001(5) | -0.001(5) | 0.007(5) |
| O9 | 1 | 0.3070(6) | 0.3225(6) | 0.7465(6) | 0.034(3) | 0.040(7) | 0.013(6) | 0.044(7) | 0.001(5) | 0.008(5) | 0.000(5) |
| O10 | 1 | 0.0708(6) | 0.3057(7) | 0.4420(6) | 0.036(3) | 0.039(6) | 0.040(8) | 0.031(6) | -0.001(6) | 0.011(5) | -0.020(6) |
| O11 | 1 | 0.1585(6) | 0.3791(7) | 0.5243(6) | 0.035(3) | 0.035(6) | 0.050(8) | 0.026(6) | -0.006(6) | 0.015(5) | -0.013(6) |
| O12 | 1 | 0.1609(6) | 0.3709(7) | 0.4088(6) | 0.040(3) | 0.040(7) | 0.059(9) | 0.023(6) | -0.005(6) | 0.014(5) | -0.031(6) |
| O13 | 1 | 0.3683(6) | 0.5170(7) | 0.7184(6) | 0.040(3) | 0.039(7) | 0.053(9) | 0.033(7) | -0.002(6) | 0.017(6) | -0.011(6) |
| O14 | 1 | 0.2744(6) | 0.4516(6) | 0.6331(6) | 0.032(3) | 0.031(6) | 0.046(8) | 0.020(6) | 0.000(5) | 0.010(5) | 0.000(6) |
| O15 | 1 | 0.3585(8) | 0.5130(8) | 0.5930(7) | 0.061(4) | 0.084(10) | 0.070(11) | 0.034(7) | -0.014(7) | 0.026(7) | -0.055(8) |
| O16 | 1 | 0.3658(7) | 0.4978(9) | 0.3322(6) | 0.062(4) | 0.060(8) | 0.108(13) | 0.023(7) | -0.003(7) | 0.022(6) | -0.050(8) |
| O17 | 1 | 0.2684(7) | 0.4440(8) | 0.3666(6) | 0.057(4) | 0.066(8) | 0.086(12) | 0.024(6) | -0.019(7) | 0.021(6) | -0.054(8) |
| O18 | 1 | 0.3601(10) | 0.5016(12) | 0.4515(7) | 0.114(9) | 0.119(13) | 0.21(2) | 0.024(7) | -0.043(10) | 0.043(8) | -0.140(15) |
| O19 | 1 | 0.0733(6) | 0.0588(6) | 0.4566(6) | 0.032(3) | 0.031(6) | 0.033(7) | 0.033(6) | -0.001(5) | 0.011(5) | 0.013(6) |
| O20 | 1 | 0.1632(6) | 0.9876(7) | 0.5406(6) | 0.036(3) | 0.037(6) | 0.054(9) | 0.021(6) | 0.004(6) | 0.017(5) | 0.011(6) |
| O21 | 1 | 0.1714(7) | 0.0008(7) | 0.4264(6) | 0.044(3) | 0.047(7) | 0.065(10) | 0.028(7) | 0.016(6) | 0.021(6) | -0.025(7) |
| O22 | 1 | 0.1291(8) | 0.3574(9) | 0.7626(7) | 0.064(4) | 0.078(10) | 0.092(12) | 0.026(7) | -0.006(8) | 0.025(7) | -0.028(9) |
| O23 | 1 | 0.3702(10) | 0.8720(12) | 0.6177(7) | 0.113(8) | 0.106(12) | 0.21(2) | 0.025(8) | 0.040(10) | 0.028(8) | 0.128(14) |
| O24 | 1 | 0.2716(7) | 0.9162(8) | 0.6490(6) | 0.046(3) | 0.051(7) | 0.065(10) | 0.030(7) | 0.008(6) | 0.024(6) | 0.029(7) |
| O25 | 1 | 0.3795(7) | 0.8702(8) | 0.3539(6) | 0.053(4) | 0.050(8) | 0.094(12) | 0.028(7) | 0.007(7) | 0.029(6) | 0.028(8) |
| O26 | 1 | 0.2857(7) | 0.9310(7) | 0.3864(6) | 0.043(3) | 0.041(7) | 0.065(10) | 0.028(6) | 0.003(6) | 0.017(5) | 0.018(7) |
| O27 | 1 | 0.3771(7) | 0.8759(10) | 0.4745(6) | 0.069(5) | 0.049(8) | 0.141(15) | 0.023(7) | 0.028(8) | 0.018(6) | 0.061(9) |
| O28 | 1 | 0.0687(7) | 0.1817(7) | 0.3165(7) | 0.045(3) | 0.046(7) | 0.037(8) | 0.065(9) | -0.005(7) | 0.037(6) | -0.002(6) |
| O29 | 1 | 0.1657(7) | 0.2439(7) | 0.2889(8) | 0.050(4) | 0.052(8) | 0.017(7) | 0.102(11) | 0.005(7) | 0.057(8) | 0.000(6) |
| O30 | 1 | 0.1738(8) | 0.1252(7) | 0.3033(8) | 0.056(4) | 0.074(9) | 0.025(8) | 0.098(11) | -0.001(7) | 0.070(9) | 0.001(7) |
| O31 | 1 | 0.8684(8) | 0.2441(7) | 0.7228(9) | 0.059(4) | 0.071(9) | 0.027(8) | 0.112(12) | -0.014(8) | 0.076(9) | -0.014(7) |
| O32 | 1 | 0.8724(6) | 0.1219(6) | 0.7168(7) | 0.038(3) | 0.032(6) | 0.022(7) | 0.065(9) | -0.015(6) | 0.020(6) | -0.004(5) |
| O33 | 1 | 0.2798(7) | 0.3202(7) | 0.2532(8) | 0.047(3) | 0.048(7) | 0.023(7) | 0.089(10) | 0.002(7) | 0.049(7) | 0.005(6) |
| O34 | 1 | 0.3869(7) | 0.9927(7) | 0.2421(8) | 0.053(4) | 0.047(8) | 0.026(8) | 0.110(12) | 0.006(7) | 0.058(8) | 0.011(6) |
| O35 | 1 | 0.3823(9) | 0.1142(7) | 0.2455(10) | 0.074(5) | 0.097(11) | 0.024(8) | 0.149(15) | -0.010(9) | 0.108(12) | 0.001(8) |
| O36 | 1 | 0.2910(7) | 0.0508(6) | 0.2736(8) | 0.051(4) | 0.057(8) | 0.015(7) | 0.105(11) | 0.020(7) | 0.058(8) | 0.016(6) |
| O37 | 1 | 0.2533(6) | 0.1906(7) | 0.8117(6) | 0.041(3) | 0.043(7) | 0.041(8) | 0.037(7) | 0.001(6) | 0.010(5) | -0.008(6) |
| O38 | 1 | 0.3551(6) | 0.1810(7) | 0.6755(6) | 0.038(3) | 0.038(6) | 0.030(7) | 0.047(7) | 0.007(6) | 0.015(5) | -0.010(6) |
| O39 | 1 | 0.3221(7) | 0.3660(8) | 0.5172(7) | 0.054(4) | 0.044(7) | 0.072(11) | 0.049(8) | -0.016(7) | 0.019(6) | 0.014(7) |
| O40 | 1 | 0.2004(8) | 0.5241(7) | 0.4757(7) | 0.056(4) | 0.075(10) | 0.046(9) | 0.035(8) | 0.009(6) | -0.002(7) | -0.002(7) |
| O41 | 1 | 0.2201(8) | -0.1530(8) | 0.4932(8) | 0.057(4) | 0.063(9) | 0.053(9) | 0.063(9) | 0.007(7) | 0.034(7) | 0.004(7) |
| O42 | 1 | 0.3272(7) | 0.0135(9) | 0.5387(7) | 0.062(4) | 0.041(7) | 0.095(12) | 0.054(9) | -0.015(8) | 0.018(6) | -0.040(8) |
| O43 | 1 | 0.3326(8) | 0.1958(8) | 0.3618(8) | 0.058(4) | 0.066(9) | 0.053(10) | 0.061(9) | -0.003(7) | 0.029(7) | -0.009(7) |
| O44 | 1 | 0.2207(8) | 0.1758(8) | 0.1673(8) | 0.061(4) | 0.078(10) | 0.050(10) | 0.064(10) | -0.005(8) | 0.037(8) | -0.005(8) |
| OW1 | 1 | 0.8589(9) | 0.3237(9) | 0.5787(9) | 0.077(5) | 0.072(10) | 0.075(12) | 0.085(12) | -0.011(10) | 0.026(9) | -0.006(9) |
| OW2 | 1 | 0.0455(6) | 0.3250(6) | 0.6026(6) | 0.029(3) | 0.031(6) | 0.032(7) | 0.029(6) | 0.002(5) | 0.014(5) | 0.000(5) |
| OW3 | 1 | 0.4754(9) | 0.6109(10) | 0.6690(10) | 0.087(5) | 0.064(10) | 0.081(13) | 0.096(13) | 0.002(10) | -0.004(9) | 0.008(9) |
| OW4 | 1 | 0.9818(10) | 0.1874(9) | 0.6572(10) | 0.083(5) | 0.116(13) | 0.059(11) | 0.115(13) | 0.008(10) | 0.095(12) | 0.015(10) |
| OW5 | 1 | 0.9296(8) | 0.1924(11) | 0.4889(8) | 0.087(6) | 0.061(9) | 0.146(18) | 0.057(10) | -0.033(11) | 0.023(8) | -0.042(11) |
| OW6 | 1 | 0.0222(11) | 0.2688(11) | 0.8279(10) | 0.104(7) | 0.105(14) | 0.113(17) | 0.076(12) | 0.012(11) | 0.002(10) | -0.047(12) |
| OW7 | 1 | 0.0286(6) | 0.3415(7) | 0.2646(7) | 0.045(3) | 0.034(6) | 0.053(9) | 0.052(8) | 0.006(6) | 0.018(6) | -0.016(6) |
| OW8 | 1 | 0.0422(6) | 0.0437(6) | 0.6113(6) | 0.032(3) | 0.024(5) | 0.038(7) | 0.033(6) | 0.011(5) | 0.009(5) | 0.006(5) |
| OW9 | 1 | 0.0365(6) | 0.0277(7) | 0.2711(7) | 0.048(3) | 0.031(6) | 0.056(9) | 0.029(7) | -0.014(7) | 0.017(6) | -0.007(6) |
| OW10 | 1 | 0.9703(7) | 0.4469(7) | 0.6521(8) | 0.057(4) | 0.059(8) | 0.028(8) | 0.099(11) | -0.002(7) | 0.048(8) | 0.002(7) |
| OW11 | 0.945 | 0.5056(10) | 0.4350(11) | 0.5773(10) | 0.090(6) | | | | | | |
| OW12 | 0.655 | 0.1943(14) | 0.1874(15) | 0.4680(15) | 0.085(8) | | | | | | |
| OW13 | 0.737 | 0.3105(14) | 0.6929(15) | 0.5604(14) | 0.098(8) | | | | | | |
| OW14 | 0.773 | 0.5644(12) | 0.6561(13) | 0.5701(12) | 0.084(7) | | | | | | |
| OW15 | 0.470 | 0.4003(19) | 0.704(2) | 0.450(2) | 0.079(10) | | | | | | |
| OW16 | 0.592 | 0.3908(15) | 0.6488(17) | 0.4922(16) | 0.076(8) | | | | | | |
| OW17 | 0.482 | 0.4544(19) | 0.332(2) | 0.6570(19) | 0.077(10) | | | | | | |
| OW18 | 0.437 | 0.481(2) | 0.283(3) | 0.646(2) | 0.093(13) | | | | | | |
| OW19 | 0.582 | 0.470(2) | 0.038(2) | 0.650(2) | 0.117(12) | | | | | | |
| OW20 | 0.431 | 0.361(3) | 0.198(3) | 0.524(3) | 0.110(15) | | | | | | |
| OW21 | 0.697 | 0.9659(13) | 0.4283(14) | 0.4895(13) | 0.078(7) | | | | | | |
| OW22 | 0.547 | 0.9317(17) | 0.3683(18) | 0.4722(17) | 0.077(9) | | | | | | |
| OW23 | 0.486 | 0.453(2) | 0.076(3) | 0.472(3) | 0.124(15) | | | | | | |
| OW24 | 0.376 | 0.501(3) | 0.155(3) | 0.427(3) | 0.098(15) | | | | | | |

which were calculated on the basis of 16 O and 1 U atoms per formula unit (apfu). The high analytical total is probably attributable to H₂O loss in the vacuum during the deposition of the conductive carbon coat and in the microprobe chamber, which

resulted in higher concentrations for the remaining constituents. Analytical data are given in Table 1.

The empirical formula (calculated on the basis of 16 O apfu) is Ca_{1.83}Na_{0.20}Sr_{0.03}U_{1.00}C_{3.00}O_{16.00}H_{10.07}, or (Ca_{1.83}Na_{0.20}Sr_{0.03})_{Σ2.05}

Table 4. Selected bond distances (Å) and cation bond-valence sums (BVS in valence units) for paramarkeyite.

| | | | | | | | |
|----------|-----------|----------|-----------|-----------------------|-----------|-----------------------|-----------|
| Ca1–O5 | 2.327(12) | Ca6–O16 | 2.310(12) | U1–O37 | 1.754(11) | U3–O41 | 1.737(14) |
| Ca1–O1 | 2.356(12) | Ca6–O32 | 2.311(12) | U1–O38 | 1.776(11) | U3–O42 | 1.795(13) |
| Ca1–O22 | 2.358(12) | Ca6–O30 | 2.328(13) | U1–O3 | 2.435(11) | U3–O23 | 2.366(12) |
| Ca1–O14 | 2.364(11) | Ca6–O21 | 2.360(11) | U1–O5 | 2.438(10) | U3–O27 | 2.412(11) |
| Ca1–O11 | 2.424(11) | Ca6–O26 | 2.404(12) | U1–O6 | 2.439(10) | U3–O20 | 2.414(10) |
| Ca1–O9 | 2.459(11) | Ca6–O36 | 2.437(12) | U1–O8 | 2.440(11) | U3–O21 | 2.420(11) |
| Ca1–OW2 | 2.514(10) | Ca6–OW9 | 2.490(12) | U1–O2 | 2.459(11) | U3–O26 | 2.445(10) |
| <Ca1–O> | 2.400 | <Ca6–O> | 2.377 | U1–O9 | 2.491(11) | U3–O24 | 2.478(11) |
| BVS | 2.12 | BVS | 2.24 | <U1–O _{ap} > | 1.765 | <U3–O _{ap} > | 1.766 |
| | | | | <U1–O _{eq} > | 2.450 | <U3–O _{eq} > | 2.423 |
| | | | | BVS | 6.18 | BVS | 6.34 |
| Ca2–O10 | 2.339(12) | Ca7–OW11 | 2.22(2) | | | | |
| Ca2–O28 | 2.359(11) | Ca7–OW16 | 2.30(3) | | | | |
| Ca2–O19 | 2.384(12) | Ca7–O18 | 2.402(16) | U2–O39 | 1.766(13) | U4–O44 | 1.763(14) |
| Ca2–OW5 | 2.394(14) | Ca7–OW3 | 2.43(2) | U2–O40 | 1.771(13) | U4–O43 | 1.772(14) |
| Ca2–O4 | 2.471(10) | Ca7–OW14 | 2.48(2) | U2–O11 | 2.380(10) | U4–O31 | 2.391(12) |
| Ca2–O8 | 2.611(11) | Ca7–O15 | 2.493(14) | U2–O18 | 2.406(12) | U4–O35 | 2.404(12) |
| Ca2–O7 | 2.653(11) | Ca7–OW11 | 2.493(19) | U2–O15 | 2.411(12) | U4–O29 | 2.417(11) |
| <Ca2–O> | 2.459 | <Ca7–O> | 2.403 | U2–O12 | 2.413(10) | U4–O30 | 2.432(11) |
| BVS | 1.89 | BVS | 2.15 | U2–O17 | 2.425(11) | U4–O36 | 2.448(12) |
| | | | | U2–O14 | 2.455(10) | U4–O33 | 2.455(12) |
| Ca3–O35 | 2.429(13) | Na7–OW3 | 2.30(2) | <U2–O _{ap} > | 1.769 | <U4–O _{ap} > | 1.768 |
| Ca3–OW6 | 2.433(18) | Na7–OW15 | 2.41(4) | <U2–O _{eq} > | 2.415 | <U4–O _{eq} > | 2.425 |
| Ca3–OW2 | 2.472(10) | Na7–O15 | 2.428(17) | BVS | 6.35 | BVS | 6.30 |
| Ca3–OW10 | 2.479(14) | Na7–O18 | 2.47(2) | | | | |
| Ca3–O31 | 2.480(12) | Na7–OW14 | 2.55(2) | C1–O1 | 1.20(2) | C7–O19 | 1.28(2) |
| Ca3–OW4 | 2.494(17) | Na7–OW13 | 2.78(3) | C1–O2 | 1.30(2) | C7–O20 | 1.28(2) |
| Ca3–OW1 | 2.516(16) | Na7–OW11 | 2.83(2) | C1–O3 | 1.30(2) | C7–O21 | 1.304(19) |
| Ca3–O22 | 2.750(14) | <Na7–O> | 2.490 | <C1–O> | 1.267 | <C7–O> | 1.288 |
| <Ca3–O> | 2.507 | BVS | 1.03 | BVS | 4.20 | BVS | 3.95 |
| BVS | 1.89 | | | | | | |
| | | | | C2–O4 | 1.249(18) | C8–O22 | 1.22(2) |
| Ca4–O29 | 2.349(12) | Ca8–OW20 | 2.25(5) | C2–O5 | 1.294(19) | C8–O23 | 1.31(2) |
| Ca4–O25 | 2.350(12) | Ca8–OW18 | 2.28(5) | C2–O6 | 1.326(19) | C8–O24 | 1.32(2) |
| Ca4–O34 | 2.351(13) | Ca8–OW19 | 2.31(4) | <C2–O> | 1.290 | <C8–O> | 1.283 |
| Ca4–O17 | 2.380(12) | Ca8–OW7 | 2.629(16) | BVS | 3.95 | BVS | 4.03 |
| Ca4–O12 | 2.394(10) | Ca8–O25 | 2.637(15) | | | | |
| Ca4–O33 | 2.428(11) | Ca8–O38 | 2.664(14) | C3–O7 | 1.261(19) | C9–O25 | 1.26(2) |
| Ca4–OW7 | 2.480(11) | Ca8–OW23 | 2.97(5) | C3–O8 | 1.283(19) | C9–O26 | 1.26(2) |
| <Ca4–O> | 2.390 | <Ca8–O> | 2.534 | C3–O9 | 1.311(18) | C9–O27 | 1.31(2) |
| BVS | 2.16 | BVS | 1.78 | <C3–O> | 1.285 | <C9–O> | 1.277 |
| | | | | BVS | 3.99 | BVS | 4.07 |
| Ca5–O13 | 2.366(11) | Na8–OW24 | 2.14(5) | | | | |
| Ca5–O6 | 2.386(11) | Na8–OW23 | 2.43(5) | C4–O10 | 1.256(19) | C10–O28 | 1.266(18) |
| Ca5–O20 | 2.394(10) | Na8–O27 | 2.44(2) | C4–O11 | 1.284(18) | C10–O29 | 1.28(2) |
| Ca5–O24 | 2.424(12) | Na8–O25 | 2.52(3) | C4–O12 | 1.289(18) | C10–O30 | 1.29(2) |
| Ca5–O2 | 2.442(11) | Na8–OW15 | 2.53(5) | <C4–O> | 1.276 | <C10–O> | 1.279 |
| Ca5–OW8 | 2.443(10) | Na8–OW20 | 2.58(5) | BVS | 4.07 | BVS | 4.05 |
| Ca5–O7 | 2.443(12) | Na8–OW18 | 2.75(5) | | | | |
| <Ca5–O> | 2.414 | <Na8–O> | 2.440 | C5–O13 | 1.261(18) | C11–O31 | 1.25(2) |
| BVS | 2.03 | BVS | 1.17 | C5–O14 | 1.283(17) | C11–O32 | 1.28(2) |
| | | | | C5–O15 | 1.319(18) | C11–O33 | 1.30(2) |
| | | Sr9–OW22 | 2.33(4) | <C5–O> | 1.288 | <C11–O> | 1.277 |
| | | Sr9–O40 | 2.40(2) | BVS | 3.96 | BVS | 4.07 |
| | | Sr9–OW21 | 2.43(3) | | | | |
| | | Sr9–O1 | 2.66(2) | C6–O16 | 1.26(2) | C12–O34 | 1.23(2) |
| | | Sr9–O11 | 2.66(2) | C6–O17 | 1.28(2) | C12–O35 | 1.29(2) |
| | | Sr9–OW10 | 2.85(2) | C6–O18 | 1.30(2) | C12–O36 | 1.309(19) |
| | | <Ca9–O> | 2.555 | <C6–O> | 1.280 | <C12–O> | 1.276 |
| | | BVS | 1.85 | BVS | 4.04 | BVS | 4.08 |

(UO₂)(CO₃)₃·5H₂O (+0.07 H). The simplified formula is (Ca,Na,Sr)₂(UO₂)(CO₃)₃·5H₂O and the ideal formula is Ca₂(UO₂)(CO₃)₃·5H₂O, which requires CaO 18.08, UO₃ 46.11, CO₂ 21.29 and H₂O 14.52, total 100 wt. %.

X-ray crystallography and structure refinement

Powder X-ray diffraction was done using a Rigaku R-Axis Rapid II curved imaging plate microdiffractometer, with

monochromatised MoK α radiation. A Gandolfi-like motion on the φ and ω axes was used to randomise the sample and observed d values and intensities were derived by profile fitting using *JADE Pro* software (Materials Data, Inc.). The powder data are presented in Supplementary Table S1. This table is deposited with the Principal Editors of *Mineralogical Magazine* and is available as Supplementary material (see below).

The single-crystal structure data were collected at room temperature using the same diffractometer and radiation noted

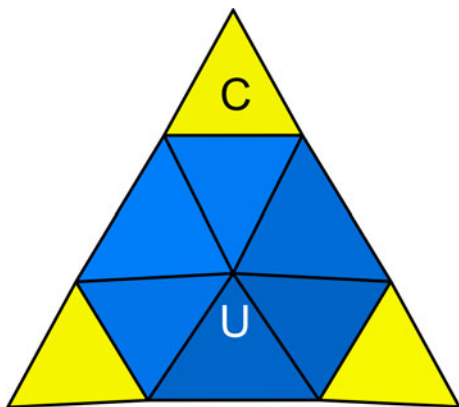


Fig. 4. The uranyl tricarbonate cluster (UTC) of formula $[(\text{UO}_2)(\text{CO}_3)_3]^{4+}$.

above. The Rigaku *CrystalClear* software package was used for processing structure data, including the application of an empirical multi-scan absorption correction using *ABSCOR* (Higashi, 2001). The structure was solved using the intrinsic phasing algorithm of the *SHELXT* program (Sheldrick, 2015a). *SHELXL-2016* (Sheldrick, 2015b) was used for the refinement of the structure. Most atoms were located and subsequently refined at full occupancies; however, several Ca and O sites exhibited disorder manifest as split sites, partial occupancies and/or prolate anisotropic displacement ellipsoids. This prompted us to perform several tests. Despite a strong indication that the data are centrosymmetric ($|E^2-1|=1.01$), seventy reflections ($I > 3\sigma I$) were found to violate systematic absence expectations for the n glide plane, and we attempted to solve the structure in the non-centrosymmetric space group $P2_1$ using a racemic twin matrix. The resulting structure, while reasonable, provides a generally

poor refinement with numerous non-positive definite anisotropic displacement ellipsoids not encountered in the $P2_1/n$ refinement.

The occupancies of the O sites in the disordered interlayer portion of the structure were refined but still exhibited unrealistically large displacement parameters ($U_{\text{eq}}/U_{\text{iso}} = 0.12\text{--}0.33 \text{ \AA}$) indicating that their refined occupancies were too high. To account for this, the occupancies for sites OW11 to OW24 were refined with U_{iso} set to 0.08. The occupancies obtained were then set in subsequent refinement cycles with U_{iso} refined. The total of the OW site occupancies provide 4.55 H_2O pfu; however, because there is additional residual electron density in the interlayer region and because the interlayer OW sites could accommodate additional occupancy, 5 H_2O pfu is used for the ideal formula.

Three pairs of split cation sites were noted in the interlayer region. Based on bond-valence sums, these sites were assigned as Ca7 and Na7 (separated by 1.18 \AA), Ca8 and Na8 (separated by 1.74 \AA) and Sr9 (separated by 2.83 \AA from another Sr9 site). The occupancies of the Ca7 and Na7 sites were refined jointly with $\text{Ca} + \text{Na} = 1$. Because of the large displacement parameters of the Ca8 and Na8 sites, joint occupancy refinement was not deemed appropriate; instead, we set the Ca8 occupancy to 0.50 Ca and the Na8 site occupancy to 0.38, which provided U_{iso} values close to 0.1 for each site. The occupancy of the Sr9 site was refined. It is worth noting that Ca is greater than Na in both the Ca7/Na7 and Ca8/Na8 paired sites and the occupancy of the Sr9 site is only 0.120(7); hence, only Ca is provided in the ideal formula. Furthermore, the site occupancies for all of the Ca, Na and Sr sites provides $(\text{Ca}_{1.76}\text{Na}_{0.21}\text{Sr}_{0.03})_{\Sigma 2.00}$ pfu, which compares very well with the analysed composition $(\text{Ca}_{1.83}\text{Na}_{0.20}\text{Sr}_{0.03})_{\Sigma 2.05}$.

The refined anisotropic displacement parameters of several of the equatorial O atoms bonded to U and C are strongly prolate. It seems likely that this is in response to the Ca disorder, i.e. the planarity of the uranyl tricarbonate (UTC) units is disordered to accommodate the disordered Ca positions. Most of the impacted

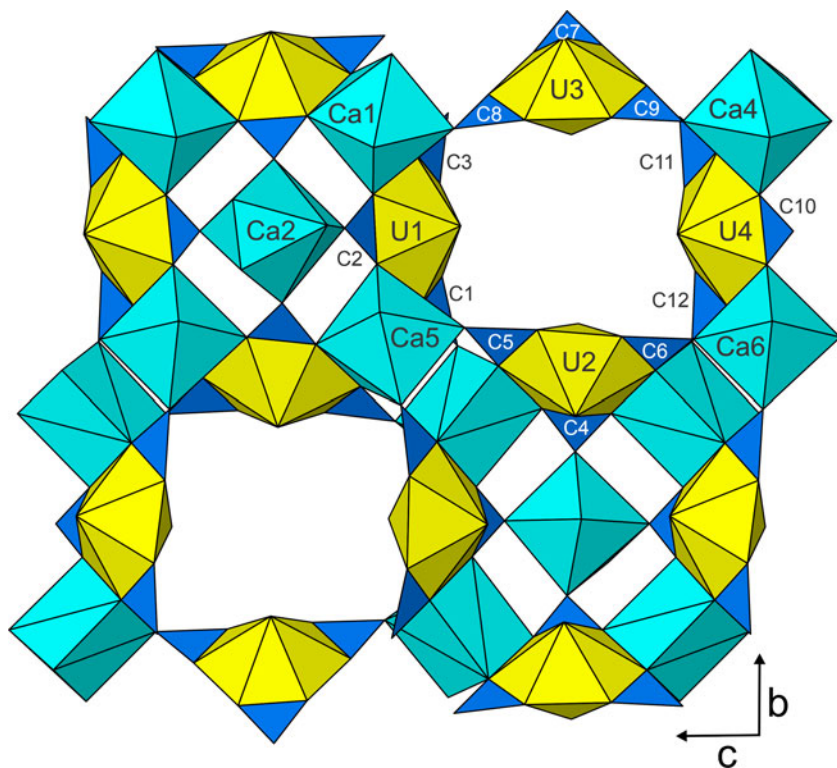


Fig. 5. The portion of the uranyl-carbonate layer that is common to the structures of markeyite, natromarkeyite, pseudomarkeyite and paramarkeyite. The cell directions and polyhedral labels apply specifically to paramarkeyite.

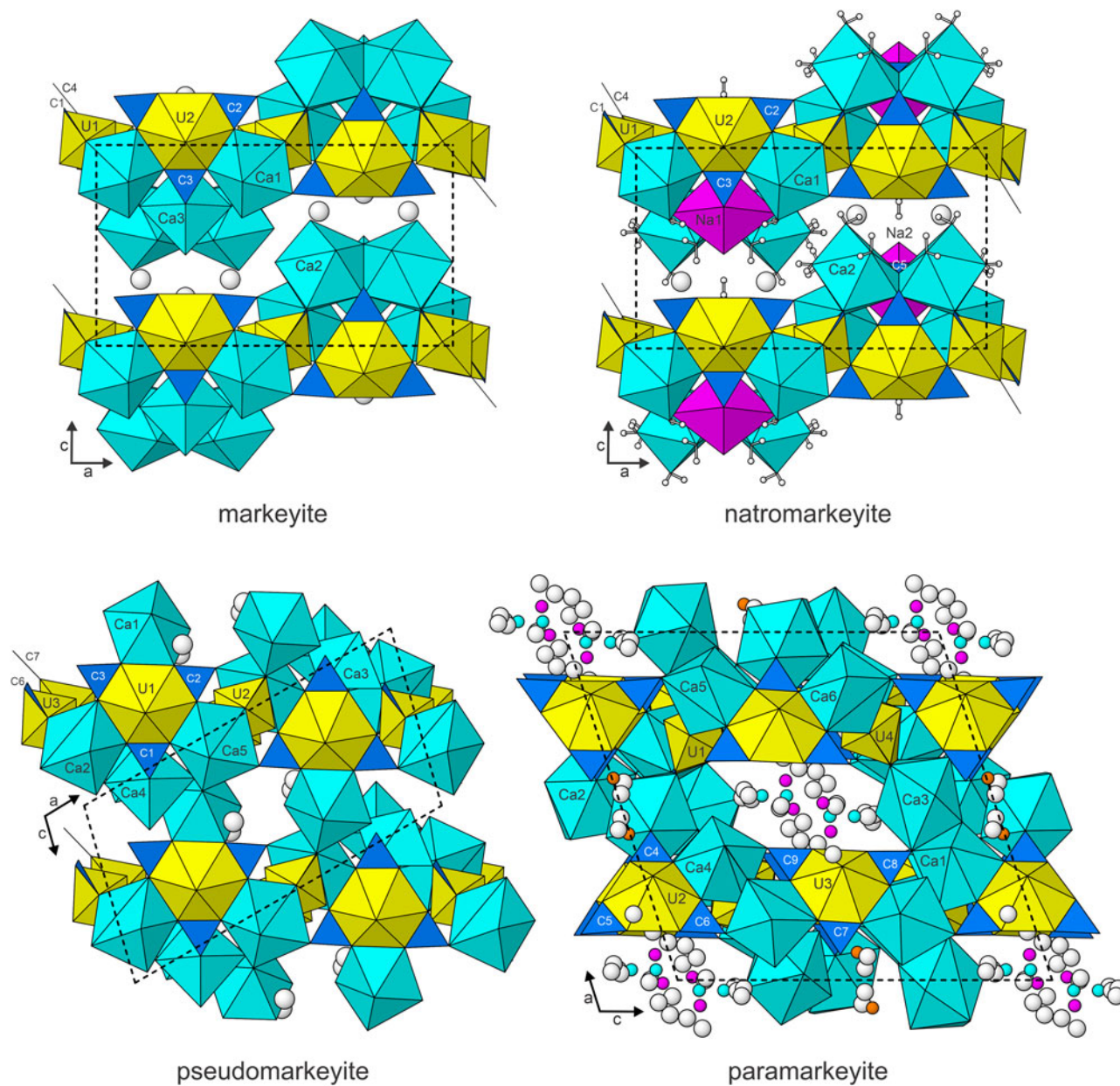


Fig. 6. The structures of paramarkeyite, pseudomarkeyite and markeyite viewed down [010]. The atoms with disordered coordinations in paramarkeyite are shown as balls: Ca7 and Ca8 are turquoise, Na7 and Na8 are pink, Sr9 is orange and all OW are white.

O atoms are in equatorial sites and are shared by Ca7/Na7 or Ca8/Na8.

Data collection and refinement details are given in Table 2, atom coordinates and displacement parameters in Table 3 and selected bond distances and cation bond-valence sums (based on bond-valence parameters from Gagné and Hawthorne, 2015) in Table 4. The crystallographic information files have been deposited with the Principal Editor of *Mineralogical Magazine* and are available as Supplementary material (see below).

Description and discussion of the structure

The four U sites (U1, U2, U3 and U4) in the structure of paramarkeyite are each surrounded by eight O atoms forming a squat UO_8 hexagonal bipyramid. These bipyramids are each

chelated by three CO_3 groups, forming uranyl tricarbonate (UTC) clusters of formula $[(UO_2)(CO_3)_3]^{4-}$ (Burns 2005; Fig. 4). Six Ca sites (Ca1, Ca2, Ca3, Ca4, Ca5 and Ca6) are not split and have well defined coordinations; all are seven coordinated except Ca2, which is eight coordinated. The Ca7, Na7, Ca8 and Na8 sites have seven-fold coordinations and the Sr9 site has six-fold coordination. It is worth noting that in the closely related mineral natromarkeyite, Na cations fill pore space between multiple UTC units, sharing oxygen atoms of outstretched CO_3 groups and apical uranyl oxygen atoms; these spaces are occupied only by O atoms of disordered H_2O groups in paramarkeyite.

The Ca–O polyhedra share edges and corners with the UTCs. The UTCs and ordered polyhedra (except the Ca3–O polyhedron) form heteropolyhedral layers parallel to {100} (Fig. 5). The heteropolyhedral layer in the structure of paramarkeyite is essentially

Table 5. Comparison of markeyite, natromarkeyite, pseudomarkeyite, paramarkeyite and liebigitte.

| | Markeyite | Natromarkeyite | Pseudomarkeyite | Paramarkeyite | Liebigite |
|-----------------|--|--|---|--|---|
| Formula* | Ca ₉ (UO ₂) ₄ (CO ₃) ₁₃ ·28H ₂ O | Na ₂ Ca ₈ (UO ₂) ₄ (CO ₃) ₁₃ ·27H ₂ O | Ca ₈ (UO ₂) ₄ (CO ₃) ₁₂ ·21H ₂ O | Ca ₈ (UO ₂) ₄ (CO ₃) ₁₂ ·20H ₂ O | Ca ₈ (UO ₂) ₄ (CO ₃) ₁₂ ·44H ₂ O |
| Symmetry | Orthorhombic, <i>Pmmn</i> | Orthorhombic, <i>Pmmn</i> | Monoclinic, <i>P2₁/m</i> | Monoclinic, <i>P2₁/n</i> | Orthorhombic, <i>Bba2</i> |
| Cell parameters | $a = 17.9688(13) \text{ \AA}$ $b = 18.4705(6) \text{ \AA}$ $c = 10.11136(4) \text{ \AA}$ | $a = 17.8820(13) \text{ \AA}$ $b = 18.3030(4) \text{ \AA}$ $c = 10.22249(3) \text{ \AA}$ | $a = 17.531(3) \text{ \AA}$ $b = 18.555(3) \text{ \AA}$ $c = 9.130(3) \text{ \AA}$ $\beta = 103.95(3)^\circ$ $V = 2882.3(13) \text{ \AA}^3$ | $a = 17.9507(7) \text{ \AA}$ $b = 18.1030(8) \text{ \AA}$ $c = 18.3688(13) \text{ \AA}$ $\beta = 108.029(8)^\circ$ $V = 5676.1(6) \text{ \AA}^3$ | $a = 16.699(3) \text{ \AA}$ $b = 17.557(3) \text{ \AA}$ $c = 13.697(2) \text{ \AA}$ $V = 4015.8 \text{ \AA}^3$ |
| Z | 2 | 2 | 2 | 4 | 2 |
| Density (meas.) | 2.68(2) g·cm ⁻³ | 2.70(2) g·cm ⁻³ | 2.88(2) g·cm ⁻³ | 2.91(2) g·cm ⁻³ | 2.41 g·cm ⁻³ |
| Optics | Biaxial (-) $\alpha = 1.538(2)$ $\beta = 1.542(2)$ $\gamma = 1.545(2)$ 2V (meas.) = 81(2)° | Biaxial (-) $\alpha = 1.528(2)$ $\beta = 1.532(2)$ $\gamma = 1.533(2)$ 2V (meas.) = 46.5(7)° | Biaxial (-) $\alpha = 1.549(2)$ $\beta = 1.556(2)$ $\gamma = 1.557(2)$ 2V (meas.) = 88(2)° | Biaxial (-) $\alpha = 1.550(2)$ $\beta = 1.556(2)$ $\gamma = 1.558(2)$ 2V (meas.) = 60(2)° | Biaxial (+) $\alpha = 1.494-1.501$ $\beta = 1.498-1.505$ $\gamma = 1.535-1.542$ 2V (meas.) = 37-42° |
| Reference | Kampf <i>et al.</i> (2017) | Kampf <i>et al.</i> (2020a) | Kampf <i>et al.</i> (2020a) | This study | Mereiter (1982); Evans and Frondel (1950) |

* To facilitate comparison, the ideal formulas are all based on 4 U apfu.

Table 6. Information measures (I_G) for markeyite, natromarkeyite, pseudomarkeyite, paramarkeyite and liebigitte including H atoms.

| Mineral | V (\AA^3) | v (\AA) | I_G (bits/atom) | $I_{G,total}$ (bits/cell) |
|-----------------|---------------------------|-------------------------|----------------------|------------------------------|
| Markeyite | 3356 | 340 | 5.83 | 1983.19 |
| Natromarkeyite | 3346 | 322 | 5.69 | 1832.56 |
| Pseudomarkeyite | 2882 | 270 | 6.22 | 1678.74 |
| Paramarkeyite | 5676 | 544 | 7.09 | 3855.58 |
| Liebigite | 4016 | 200 | 5.66 | 1132.77 |

identical to the layers in the structures of markeyite, natromarkeyite and pseudomarkeyite. Viewed down the **b** axis (Fig. 6), the structures are seen to differ in the arrangement of additional Ca–O polyhedra (and a disordered CO₃ group in the markeyite and natromarkeyite structures). We conjecture that the disorder in the interlayer region of the paramarkeyite structure and the different arrangement of non-layer polyhedra (including the Ca3–O polyhedron) is driven by the presence of minor Na and Sr, which can only be accommodated by splitting the cation sites.

The structure of liebigitte, Ca₂(UO₂)(CO₃)₃·11H₂O (Mereiter, 1982), contains the same structural components as those in the structures of markeyite, natromarkeyite, pseudomarkeyite and paramarkeyite. The same types of polyhedral linkages occur in all five structures, where the Ca–O polyhedra link UTCs forming heteropolyhedral layers. In the structure of liebigitte, as in that of markeyite, these layers link to one another and to interlayer H₂O groups only *via* hydrogen bonds. However, the topology of the layer in liebigitte is quite different from those in markeyite, natromarkeyite, pseudomarkeyite and paramarkeyite. Selected data for markeyite, natromarkeyite, pseudomarkeyite, paramarkeyite and liebigitte are compared in Table 5.

The structures of the aforementioned minerals were further evaluated with regard to their structural complexities (after Krivovichev 2012, 2013, 2014, 2018) (Table 6). Paramarkeyite, with a complexity of 3855.58 bits/cell, is classified as very complex. It is not only the most complex within this group of related minerals, but it is the fourth most complex uranyl carbonate mineral known (see Gurzhiy *et al.*, 2021). It is noteworthy that paramarkeyite also has the greatest density of the five related minerals listed in Tables 5 and 6; of the five, it has the lowest H₂O content and thus the structure is the most densely packed regardless of having the largest unit-cell volume in the group.

Acknowledgements. Aaron Lussier and an anonymous reviewer are thanked for their comments on the manuscript. Comments by Structures Editor Peter Leverett were particular helpful in improving the structure refinement. A portion of this study was funded by the John Jago Trelawney Endowment to the Mineral Sciences Department of the Natural History Museum of Los Angeles County. This research was also financially supported by the Czech Science Foundation (project 20-11949S to JP) and by the Operational Program – Research, Development and Education (OP VVV) (project Geobarr CZ.02.1.01/0.0/0.0/16_026/0008459 to RS).

Supplementary material. To view supplementary material for this article, please visit <https://doi.org/10.1180/mgm.2021.100>

References

Anderson A., Chieh Ch., Irish D.E. and Tong J.P.K. (1980) An X-ray crystallographic, Raman, and infrared spectral study of crystalline potassium uranyl carbonate, K₄UO₂(CO₃)₃. *Canadian Journal of Chemistry*, **58**, 1651–1658.

- Bartlett J.R. and Cooney R.P. (1989) On the determination of uranium-oxygen bond lengths in dioxouranium(VI) compounds by Raman spectroscopy. *Journal of Molecular Structure*, **193**, 295–300.
- Burns P.C. (2005) U⁶⁺ minerals and inorganic compounds: insights into an expanded structural hierarchy of crystal structures. *The Canadian Mineralogist*, **43**, 1839–1894.
- Čejka J. (1999) Infrared and thermal analysis of the uranyl minerals. Pp. 521–622 in: *Uranium: Mineralogy, Geochemistry, and the Environment* (P.C. Burns and R. Finch, editors). Reviews in Mineralogy, **38**. Mineralogical Society of America, Washington, DC.
- Čejka J. (2005) Vibrational spectroscopy of the uranyl minerals – infrared and Raman spectra of the uranyl minerals. II. Uranyl carbonates. *Bulletin mineralogicko-petrologického oddělení Národního muzea (Praha)*, **13**, 62–72 [and references therein, in Czech].
- Chenoweth W.L. (1993) The geology and production history of the uranium deposits in the White Canyon Mining District, San Juan County, Utah. *Utah Geological Survey Miscellaneous Publication*, 93–3.
- Evans Jr H.T. and Frondel C. (1950) Studies of uranium minerals (II): Liebigite and uranohallite. *American Mineralogist*, **35**, 251–254.
- Gagné O.C. and Hawthorne F.C. (2015) Comprehensive derivation of bond-valence parameters for ion pairs involving oxygen. *Acta Crystallographica*, **B71**, 562–578.
- Gurzhiy V.V., Kalashnikova S.A., Kuporev I.V. and Plášil J. (2021) Crystal chemistry and structural complexity of the uranyl carbonate minerals and synthetic compounds. *Crystals*, **11**, 704.
- Higashi T. (2001) *ABSCOR*. Rigaku Corporation, Tokyo.
- Kampf A.R., Plášil J., Kasatkin A.V., Marty J. and Čejka J. (2017) Klaprothite, péligotite and ottohahnite, three new sodium uranyl sulfate minerals with bidentate UO₇–SO₄ linkages from the Blue Lizard mine, San Juan County, Utah, USA. *Mineralogical Magazine*, **80**, 753–779.
- Kampf A.R., Plášil J., Kasatkin A.V., Marty J. and Čejka J. (2018) Markeyite, a new calcium uranyl tricarbonato mineral from the Markey mine, San Juan County, Utah, USA. *Mineralogical Magazine*, **82**, 1089–1100.
- Kampf A.R., Olds T.A., Plášil J., Marty J. and Perry S.N. (2019a) Feynmanite, a new sodium–uranyl–sulfate mineral from Red Canyon, San Juan County, Utah, USA. *Mineralogical Magazine*, **83**, 153–160.
- Kampf A.R., Plášil J., Kasatkin A.V., Nash B.P. and Marty J. (2019b) Magnesioleydetite and straßmannite, two new uranyl sulfate minerals with sheet structures from Red Canyon, Utah. *Mineralogical Magazine*, **83**, 349–360.
- Kampf A.R., Plášil J., Olds T.A., Nash B.P., Marty J. and Belkin H.E. (2019c) Meyrowitzite, Ca(UO₂)(CO₃)₂·5H₂O, a new mineral with a novel uranyl-carbonate sheet. *American Mineralogist*, **103**, 603–610.
- Kampf A.R., Olds T.A., Plášil J., Burns P.C. and Marty J. (2020a) Natromarkeyite and pseudomarkeyite, two new calcium uranyl carbonate minerals from the Markey mine, San Juan County, Utah, USA. *Mineralogical Magazine*, **84**, 753–765.
- Kampf A.R., Plášil J., Nash B.P., Němec I. and Marty J. (2020b) Uroxite and metauroxite, the first two uranyl-oxalate minerals. *Mineralogical Magazine*, **84**, 131–141.
- Kampf A.R., Olds T.A., Plášil J., Nash B.P. and Marty J. (2021a) Uranoclite, a new uranyl-chloride mineral from the Blue Lizard mine, San Juan County, Utah, USA. *Mineralogical Magazine*, **85**, 438–443.
- Kampf A.R., Olds T.A., Plášil J., Burns P.C., Škoda R. and Marty J. (2021b) Paramarkeyite, IMA 2021-024. CNMNC Newsletter 62. *Mineralogical Magazine*, **85**, <https://doi.org/10.1180/mgm.2021.62>
- Koglin E., Schenk H.J. and Schwochau K. (1979) Vibrational and low temperature optical spectra of the uranyl tricarbonato complex [UO₂(CO₃)₃]⁴⁻. *Spectrochimica Acta*, **35A**, 641–647.
- Krivovichev S.V. (2012) Topological complexity of crystal structures: Quantitative approach. *Acta Crystallographica*, **A68**, 393–398.
- Krivovichev S.V. (2013) Structural complexity of minerals: information storage and processing in the mineral world. *Mineralogical Magazine*, **77**, 275–326.
- Krivovichev S.V. (2014) Which inorganic structures are the most complex? *Angewandte Chemie, International Edition English*, **53**, 654–661.
- Krivovichev S.V. (2018) Ladders of information: What contributes to the structural complexity of inorganic crystals. *Zeitschrift für Kristallographie*, **233**, 155–161.
- Libowitzky E. (1999) Correlation of O–H stretching frequencies and O–H...O hydrogen bond lengths in minerals. *Monatshefte für Chemie*, **130**, 1047–1059.
- Lussier A.J., Lopez R.A.K. and Burns P.C. (2016) A revised and expanded structure hierarchy of natural and synthetic hexavalent uranium compounds. *The Canadian Mineralogist*, **54**, 177–283.
- Mandarino J.A. (1976) The Gladstone–Dale relationship – Part 1: derivation of new constants. *The Canadian Mineralogist*, **14**, 498–502.
- Mandarino J.A. (2007) The Gladstone–Dale compatibility of minerals and its use in selecting mineral species for further study. *The Canadian Mineralogist*, **45**, 1307–1324.
- Mereiter K. (1982) The crystal structure of liebigite, Ca₂UO₂(CO₃)₃·~11 H₂O. *Tschermaks Mineralogische und Petrographische Mitteilungen*, **30**, 277–288.
- Merlet C. (1994) An accurate computer correction program for quantitative electron probe microanalysis. *Microchimica Acta*, **114/115**, 363–376.
- Olds T., Sadegaski L.R., Plášil J., Kampf A.R., Burns P., Steele I.M., Marty J., Carlson S.M. and Mills O.P. (2017) Leószilárdite, the first Na, Mg-containing uranyl carbonate from the Markey mine, San Juan County, Utah, USA. *Mineralogical Magazine*, **81**, 743–754.
- Sheldrick G.M. (2015a) *SHELXT* – Integrated space-group and crystal-structure determination. *Acta Crystallographica Section A*, **A71**, 3–8.
- Sheldrick G.M. (2015b) Crystal structure refinement with *SHELX*. *Acta Crystallographica*, **C71**, 3–8.